



Effects of plasma treatment to nanofibers on initial cell adhesion and cell morphology



Wei Liu^{a,b}, Jianchao Zhan^{b,c}, Yan Su^{a,b}, Tong Wu^b, Chunchen Wu^b,
Seeram Ramakrishna^d, Xiumei Mo^{a,b,*}, Salem S. Al-Deyab^e, Mohamed El-Newehy^{e,f}

^a State Key Lab for Modification of Chemical Fiber & Polymer Materials, College of Material Science and Engineering, Donghua University, Shanghai 201620, PR China

^b Biomaterials and Tissue Engineering Lab, College of Chemistry, Chemical Engineering and Biotechnology, Donghua University, Shanghai 201620, PR China

^c College of Materials and Textile Engineering, Jiaying University, Zhejiang 314001, PR China

^d HEM Laboratories, National University of Singapore, Nanoscience & Nanotechnology Initiative (NUSNNI), 2 Engineering Drive 3, 117576, Singapore

^e Department of Chemistry, College of Science, King Saud University, Riyadh 11451, Saudi Arabia

^f Department of Chemistry, Faculty of Science, Tanta University, Tanta 31527, Egypt

ARTICLE INFO

Article history:

Received 10 April 2013

Received in revised form 8 August 2013

Accepted 26 August 2013

Available online xxx

Keywords:

Plasma treatment
Hydrophilicity
Initial cell adhesion
Electrospinning
Nanofibrous mat

ABSTRACT

Poly-L-lactic acid (PLLA) nanofibers were fabricated by electrospinning and treated with O₂ plasma. The surface properties of PLLA nanofibers before and after plasma treatment were characterized by water contact angle measurement and X-ray photoelectron spectroscopy (XPS). It was found that the hydrophilicity of PLLA nanofibers was improved and the amount of oxygen-containing groups increased after plasma treatment. Initial cell adhesion was evaluated by cell capture efficiency based on the cell count method. The results showed that initial porcine mesenchymal stem cells (pMSCs) adhesion to plasma-treated nanofibers was significantly enhanced. Moreover, the morphology of pMSCs on PLLA nanofibers (PLLA NFS) and plasma-treated PLLA nanofibers (P-PLLA NFS) were observed by scanning electron microscope (SEM) after 10 min, 20 min, 30 min and 60 min cell adhesion. It was found that plasma treatment to electrospun nanofibers had a great effect on pMSCs morphology at earlier time points. Therefore, plasma treatment is an efficient surface modification strategy to improve cell adhesion in earlier culture time intervals. It may be a promising method in the design of novel tissue-engineered scaffolds.

© 2013 Elsevier B.V. All rights reserved.

1. Introduction

Large quantities of polymeric biomaterials employed in tissue engineering have been designed and synthesized in recent years. Synthetic polymeric biomaterials such as polycaprolactone (PCL) and Poly(L-lactic acid) (PLLA) have been known to have poor hydrophilicity and weak biocompatibility when compared to natural polymeric biomaterials. Plasma treatment is a promising method to modify the surface of materials and has been employed in tissue engineering to make suitable implants and scaffolds in recent years [1,2]. Different functional chemical groups could be introduced onto the surface of materials by different plasma modifying strategies, and the surface properties of materials such as wettability, surface energy and surface roughness were changed [3,4].

Poly(L-lactic acid) (PLLA) is a synthetic biodegradable polymer which has been approved by US Food and Drug Administration for clinical use. But scaffolds derived from PLLA lack bioactive signals for cell recognition and the surface of PLLA scaffold is hydrophobic [5]. There are many surface modification methods to solve these problems; plasma treatment is one such promising approach [6]. The effect of plasma-treated PLLA surface on cell adhesion has been widely investigated [7]. Different plasma strategies and cells were employed in those studies, but the results were similar. It was found that plasma-treated PLLA scaffolds showed improved surface hydrophilicity and better biocompatibility [8–11].

It has been confirmed that cell adhesion to materials surface (cell capture efficiency) played an important role in cell growth, spreading, proliferation and differentiation [12,13]. As cell adhesion on material surface is crucial for tissue formation *in vivo*, it is important to know how cells can interact with material surface *in vitro*. A better understanding of cell adhesion on material surface at the initial adhesion stage is helpful to the design of ideal scaffold for tissue engineering. Moreover, the study of initial cell adhesion can explore the possibility of an attractive therapeutic approach in which scaffold with an enriched population of target cells could be

* Corresponding author at: Biomaterials and Tissue Engineering Lab, College of Chemistry, Chemical Engineering and Biotechnology, Donghua University, Shanghai 201620, PR China. Tel.: +86 2167792653.

E-mail address: xmm@dhu.edu.cn (X. Mo).

achieved. The hope of seeding the cells directly on scaffold *in situ* at the operating theater may be realized.

But as of current literature on cell adhesion to scaffolds after the cells have been seeded on scaffolds for hours or longer culture time [14,15], there are no reports on cell adhesion of plasma-treated materials, and cell morphology in an earlier time period such as in 10 min or 20 min. As it has been widely investigated that cell adhesion to plasma-treated surface was improved in hours or longer culture time, the aim of this work is to investigate mesenchymal stem cell (MSC) adhesion behaviors on electrospun PLLA nanofibers treated with plasma at earlier time interval. The surface properties of electrospun nanofibers were characterized by water contact angle and X-ray photoelectron spectroscopy (XPS). Initial cell adhesion was evaluated by the cell count method and the morphology of pMSCs on plasma-treated nanofibers was observed by scanning electron microscope.

2. Experimental

2.1. Materials

The material PLLA and the solvent 1,1,1,3,3,3-hexafluoro-2-isopropyl alcohol (HFIP) were purchased from Sigma–Aldrich Chemical Company (St. Louis, Missouri, USA). Essential Medium Alpha medium (α -MEM), fetal bovine serum, penicillin & streptomycin and 4', 6-diamidino-2-phenylindole (DAPI) were purchased from Invitrogen Corporation (USA). All products were used without further purification.

2.2. Preparation of PLLA nanofibers

The PLLA nanofibers (PLLA NFS) were prepared by the electrospinning process. The electrospinning solution of PLLA was

prepared by dissolving a 3% (w/v) PLLA solution in HFIP. Electrospinning was done by using a 5 mL standard syringe with a blunt-ended needle. The syringe was located in a syringe pump (789100C, Cole-Parmer, USA) and dispensed at a rate of 1.0 mL/h. A voltage of 20 kV was applied. The distance between the collector and needle was 12 cm. The nanofibrous membranes were dried under vacuum at room temperature overnight.

2.3. Plasma treatment of PLLA nanofibers

Electrospun PLLA nanofibrous scaffolds were treated 60 s using PDC-002 plasma (USA) in the presence of oxygen. The chamber was evacuated to less than 10 mTorr before it was filled with gas, followed by generation of glow-discharged plasma for a pre-determined time.

2.4. Scanning electron microscopy

The morphology of PLLA NFS and plasma-treated PLLA nanofibers (P-PLLA NFS) was characterized by a JSM-5600 scanning electronic microscope (SEM) (Japan). The samples were mounted on aluminum holders before sputter-coated with gold platinum for better conductivity, and then the SEM images were taken.

2.5. X-ray photoelectron spectroscopy measurement

X-ray photoelectron spectroscopy (XPS) was performed with a PH1 1500C Spectrometer (Japan) in order to determine the surface chemical components of PLLA NFS and P-PLLA NFS. The X-ray source was a magnesium anode at 15 kV and 400 W. The relative amounts of differently bound carbons were determined from high

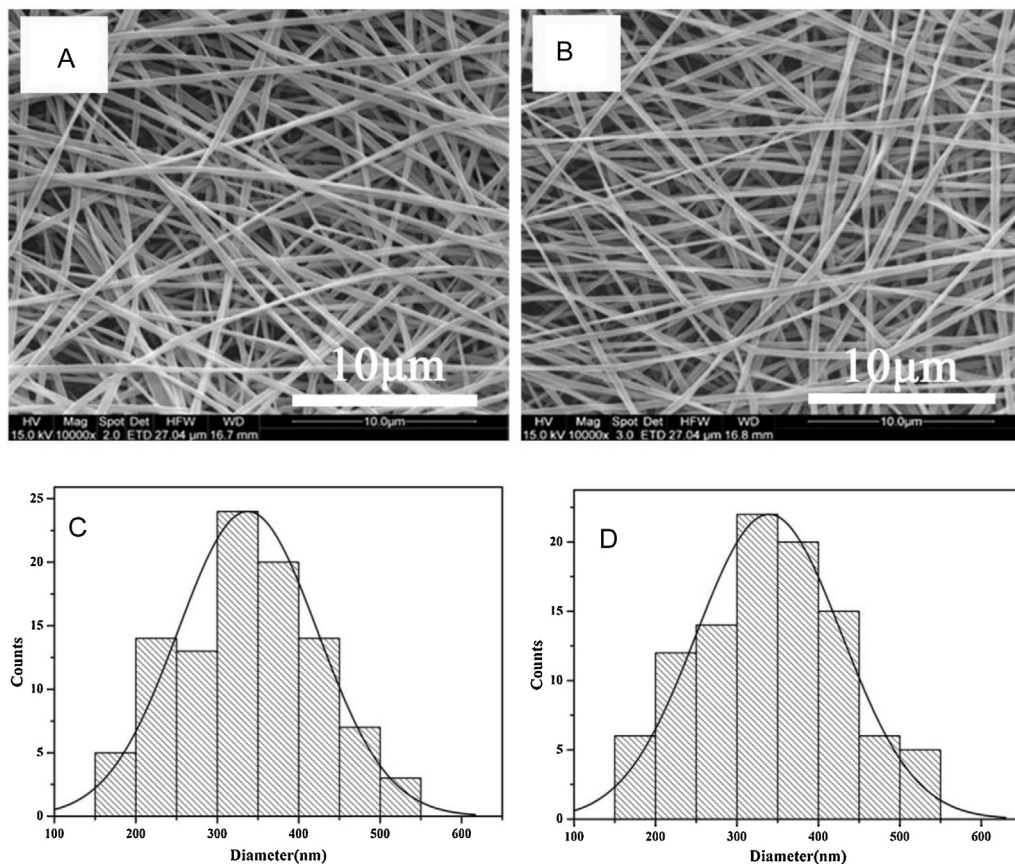


Fig. 1. SEM images of PLLA NFS (A) and P-PLLA NFS (B); The diameter distribution of PLLA NFS (C) and P-PLLA NFS (D).

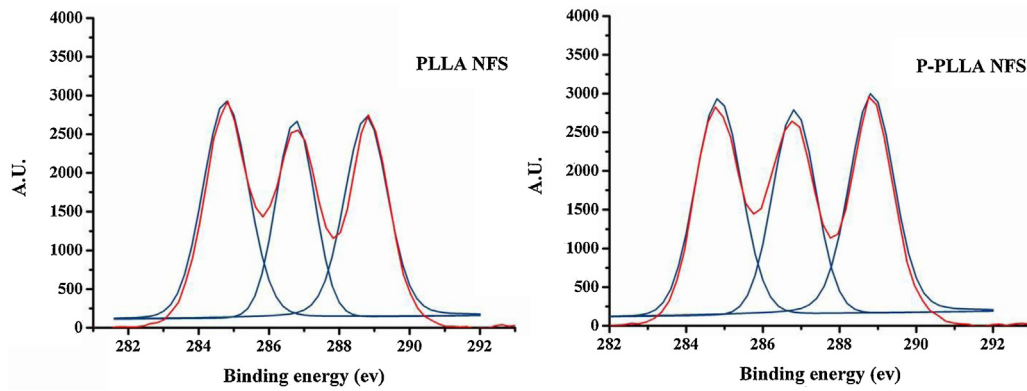


Fig. 2. XPS C1s spectra of PLLA NFS and P-PLLA NFS.

resolution C 1s spectra by using symmetrical Gaussian peak shapes and integrated background subtraction.

2.6. Water contact angles measurement

The contact angle of water droplets contacting the samples was measured using an OCA40 contact angle measurement instrument (Germany). Deionized water was used for the measurement and 6 independent measurements were averaged for each sample.

2.7. Isolation and culture of porcine mesenchymal stem cells

Bone marrow aspirates were obtained from the femoral shaft of a 6 month old female pig. Porcine mesenchymal stem cells (pMSCs) were isolated by a centrifugation method. Briefly, 18 mL porcine bone marrow aspirate and 2 mL heparin solution were mixed in 50 mL centrifuge tube and centrifuged at $400 \times g$ for 30 min at room temperature. Concentrated leukocyte band was discarded. 5 mL cell suspension and 10 mL α -MEM supplemented with 10% fetal bovine serum (FBS) were plated in 75 cm² plate. After 24 h, unattached cells were washed off the flask during medium change. Adherent fibroblast-like cells were allowed to grow for 14 days and medium supplemented with 10% FBS and 1% penicillin–streptomycin was replaced every third day. Cells were detached by trypsin/EDTA (Cell Applications, USA) and passaged after they reached near confluence (80–90%). FTIC-labeled CD90 as a specific marker expressed by bone marrow mesenchymal stem cells was used to identify pMSCs.

2.8. Initial pMSCs adhesion

Initial cell adhesion was evaluated by cell capture efficiency based on the cell count method. pMSCs at passage 3 were seeded on tissue culture polystyrene (TCP), P-PLLA NFS and PLLA NFS at the density of 1×10^4 cells/mL and incubated at room temperature for 10 min, 20 min, 30 min and 60 min. At the end of the incubation period, the solutions containing the unattached cells were discarded and each well containing the test samples was washed three times with PBS. For the purpose of cell counting, the nuclei of adhered pMSCs were stained with DAPI. Each test sample was photographed using a fluorescence microscope (Leica DM IRB) at 100 times magnification. For each test sample, the number of cells in 5 areas (top, center, bottom, left and right portions of the culture well) was counted based on the nuclei counting, then pMSCs capture efficiency was calculated by the following equation:

$$\text{Cell capture efficiency} = \frac{N_0 S}{N S_0} 100\%$$

where N and N_0 are the initial cell number seeded on sample and average cell number attaching on chosen places, respectively, and S

and S_0 are the total surface area of the sample and the surface area of a chosen place, respectively.

2.9. pMSCs morphology

Cell density of 1×10^4 cells/mL was seeded on TCP, P-PLLA NFS and PLLA NFS for 10 min, 20 min, 30 min and 60 min. Nanofibers with cells were fixed in 4% paraformaldehyde solution for 30 min at room temperature, then they were dehydrated with increasing concentrations of ethanol (50%, 70%, 95%, 100%) for five cycles. Samples were subsequently air-dried overnight and observed by SEM.

2.10. Statistical analysis

Data are presented as means \pm standard deviation. Statistical comparisons were performed using Student's *t*-test. *P* values <0.01 were considered significant.

3. Results and discussion

3.1. Surface characterizations of nanofibers before and after plasma treatment

As shown in Fig. 1A, uniform morphology of PLLA NFS was observed. There were no obvious changes after plasma treatment

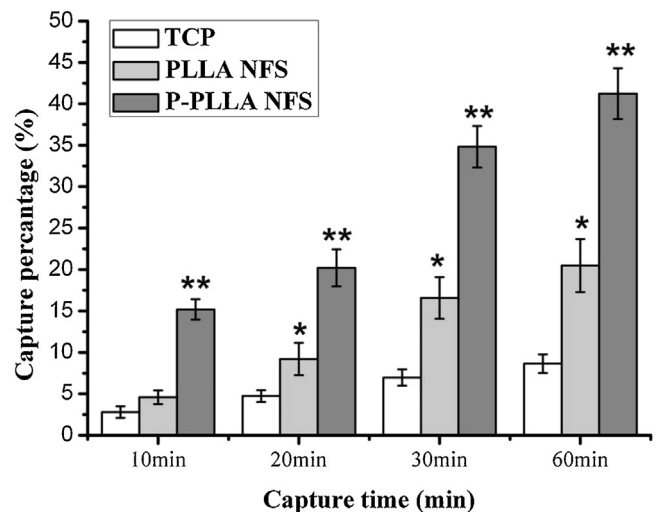


Fig. 3. Capture efficiency of pMSCs on control, PLLA NFS and P-PLLA NFS characterized by cell count method.

Table 1
Fraction of carbon functional groups from high resolution C1s XPS peaks.

| Sample | C–C (%)~284.8 eV | C–O (%)~286.8 eV | O=C–O (%)~288.9 eV |
|------------|------------------|------------------|--------------------|
| PLLA NFS | 37.68 | 27.95 | 34.37 |
| P-PLLA NFS | 34.36 | 29.82 | 35.82 |

(Fig. 1B). The diameters of nanofibers before and after plasma treatment were between 150 nm and 550 nm (Fig. 1C and D). The average diameter of PLLA NFS and P-PLLA NFS was 337 ± 85 nm and 339 ± 89 nm, respectively. The study showed that plasma treatment had no significant effect on the topological structure of electrospun nanofibers if the diameter of electrospun nanofibers was larger than 80 nm [16]. Only smooth surface morphology was observed by SEM in our results which indicated that plasma treatment had no obvious effect on the surface morphology of electrospun nanofibers.

XPS was utilized to characterize the surface chemical composition of PLLA NFS and P-PLLA NFS. High resolution XPS C1s spectra

of PLLA NFS and P-PLLA NFS are shown in Fig. 2 and the fractions of different carbon functional groups are exhibited in Table 1. The C1s spectra of the PLLA NFS before and after plasma treatment reveal the presence of three peaks corresponding to C–C (284.8 eV), C–O (286.8 eV), and O=C–O (288.9 eV) bonds. After plasma treatment, the saturated hydrocarbon C–C bond decreased 3.31%, and the concentration of C–O bond and O=C–O bond increased 1.87% and 1.45%, respectively. The decrease of carbon content and the increase of oxygen content were contributed to the introduction of oxygen-containing polar groups on the surface of electrospun nanofibers by plasma treatment.

As shown in Table 2, plasma treatment induced significant change on water contact angle of nanofibers. Water contact angle of PLLA NFS is $128.2 \pm 2.3^\circ$. It shows that PLLA is a hydrophobic polymer. After plasma treatment, it decreased to $48.5 \pm 3.3^\circ$. It indicated that the surface of plasma-treated PLLA NFS became more hydrophilic. The introduction of oxygen-containing polar groups on the surface of nanofibers resulted in the significant change of hydrophilicity, which has been confirmed by multiple studies [7,17].

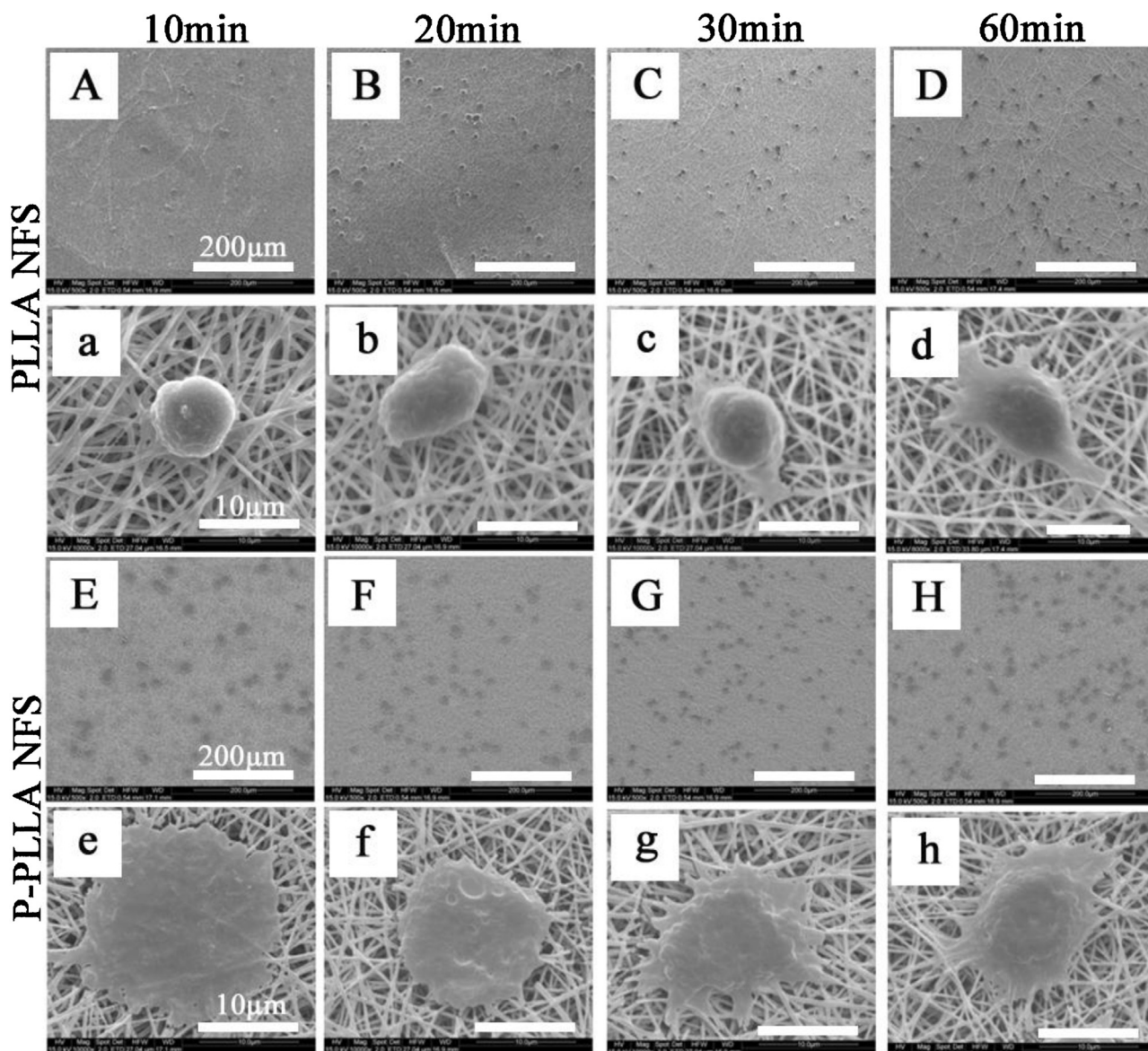




Fig. 4. SEM images of pMSCs on P-PLLA NFS and PLLA NFS. (A–D) pMSCs on PLLA NFS after cultured for 10 min, 20 min, 30 min, 60 min, respectively; (E–H) pMSCs on P-PLLA NFS after cultured for 10 min, 20 min, 30 min, 60 min, respectively; (a–d) higher magnification for (A–D), respectively; (e–h) higher magnification for (E–H), respectively.

Table 2
water contact angle of PLLA NFS and P-PLLA NFS.

| | PLLA NFS | P-PLLA NFS |
|-------------------------|---|---|
| Water contact angle (°) | 128.2 ± 2.3 | 48.5 ± 3.3 |
| Schematic diagram |  |  |

3.2. Initial cell capture efficiency and cell morphology

Cell capture efficiency was used to evaluate the initial adhesion ability of pMSCs on TCP, PLLA NFS and P-PLLA NFS at earlier time points (10 min, 20 min 30 min and 60 min). As shown in Fig. 3, pMSCs capture efficiencies on PLLA NFS were significantly higher than that on TCP at 20 min, 30 min and 60 min ($*p < 0.01$). Moreover, pMSCs capture efficiencies on P-PLLA NFS were significantly higher than that on TCP and PLLA NFS at all time points ($**p < 0.01$). At 10 min, cell capture efficiency on P-PLLA NFS was three times higher than those on PLLA NFS. At 30 min, it was close to 35%, which was five times higher than that at 10 min. A study showed that electrospun nanofibers mimicing natural extracellular matrix (ECM) could promote the cell capture ability in earlier time points at room temperature [18]. Our results correspond to this study. More importantly, cell capture ability of plasma-treated nanofibers was significantly improved when it was compared with untreated nanofibers. pMSCs attachment behaviors on PLLA NFS and P-PLLA NFS were studied at different culture time points (10 min, 20 min 30 min and 60 min) by SEM. As shown in Fig. 4A–H, as the culture time lasted longer, the number of adhered pMSCs on PLLA NFS and P-PLLA NFS increased. As shown in Fig. 4a–h, pMSCs on PLLA NFS and P-PLLA NFS at different culture time points showed different morphology. Ball-shaped morphology of pMSCs on PLLA NFS was observed at 10 min and 20 min culture time points (Fig. 4a and b). pMSCs on PLLA NFS slightly stretched as the cultur time reached 30 min (Fig. 4c). As shown in Fig. 4e and f, pMSCs on P-PLLA NFS showed two-dimension planar morphology and integrated well with P-PLLA NFS at 10 min and 20 min culture time points.

After adhesion to P-PLLA NFS for 30 min, pMSCs showed three-dimension and stretched morphology (Fig. 4g and h). Furthermore, the integration between pMSCs and P-PLLA NFS was much better.

In the process of cell adhesion to ECM, receptors play an important role. one class of receptors called “integrins” can bind to specific binding site. They distribute randomly on the outer wall of the cell. Cells can sense their surroundings through protrusions and receptors response occur to bind to specific sites [19,20]. Integrins such as $\alpha\beta1$ (VLA4) can mediate all adhesive phases which are arrest adhesion, and focal adhesion [21,22]. The clustering of the integrin or affinity modulation can trig the arrest phase. The focal adhesion is comprised of integrins as the major adhesion receptors and associated cytoplasmic plaque proteins which are the major sites of actin filament attachment at the contact surface [21]. As soon as the receptors bind to the ECM molecules, a change in cytoplasmic domain of the receptors occurs, which associates with the cytoskeleton at focal adhesion sites [23]. In our case, as shown in Fig. 5A, the surface of PLLA NFS is hydrophobic and lacks bioactive groups. It's difficult for integrin receptors to find suitable bind sites to bind to when the arrest adhesion occurs. It resulted in the ball-shaped cell morphology at the 20 min interval. As the focal adhesion occurred after 20 min, the cells slightly stretched on the nanofibrous surface and poor integration between cells and nanofibers was observed (Fig. 5B). Plasma treatment introduced oxygen-containing polar groups to the surface of electrospun nanofibers [17]. These oxygen-containing polar groups promoted the hydrophilicity of PLLA NFS and provided enough specific binding sites for integrin receptors to bind to (Fig. 5C). This

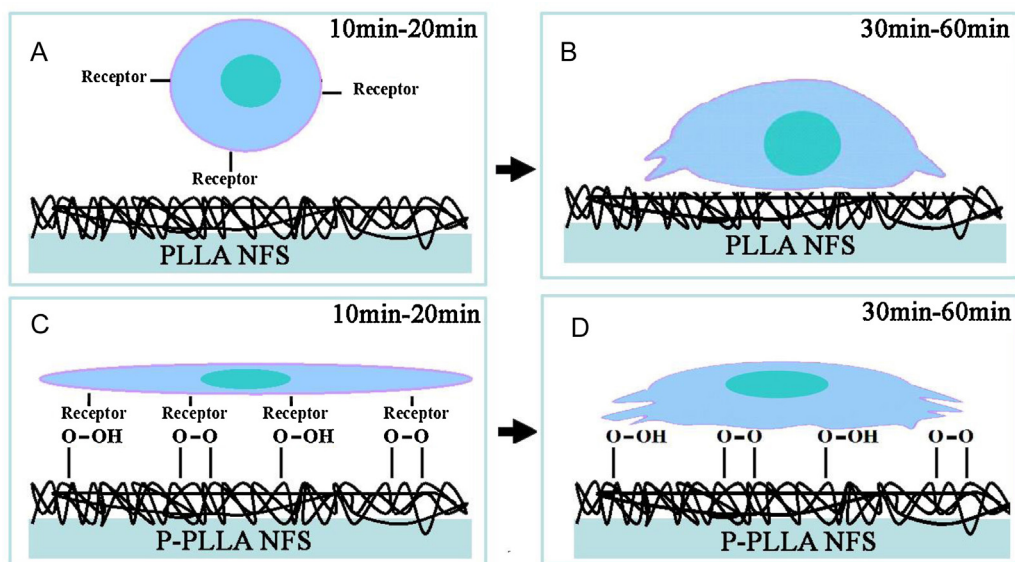


Fig. 5. Schematic diagram of cell adhesion behaviors on PLLA NFS (A and B) and P-PLLA NFS (C and D) at different time intervals.

might be an explanation for the two-dimension planar morphology of cells on P-PLLA NFS at the 20 min interval. Cell-generated tensile forces are resisted by ECM molecules and isometric tension is increased within the cell when its surface receptors bind to ECM. Forces resisted by receptors may act as feedback to change cytoskeletal filament assembly [24]. The reassembly of cytoskeletal filament might cause the change from two-dimension cell morphology to three-dimension in 30 min. Because of the improved hydrophilicity and increased oxygen-containing polar groups on P-PLLA NFS, the cells stretched and integrated well with nanofibrous surface (Fig. 5D).

Our results exhibit that cell adhesion behaviors can be significantly altered in shorter adhesion time period and cell capture efficiency for plasma-treated nanofibers was great higher than that for untreated nanofibers in one hour. Inducing oxygen-containing functional groups to the surface of nanofibers by oxygen plasma treatment significantly modified the hydrophilicity of nanofibers which might improve cell capture efficiency and cause a change in cell morphology in 60 min.

4. Conclusion

In this study, we demonstrate the effects of plasma treatment to polymeric nanofibers on their surface properties and the effects of plasma-treated nanofibers on initial stem cell adhesion behaviors. Oxygen plasma treatment introduced oxygen-containing polar groups to the surface of PLLA nanofibers, and the hydrophilicity of PLLA nanofibers was significantly improved. It was also observed that initial stem cell adhesion on plasma-treated nanofibers was significantly enhanced. The morphology of pMSCs in earlier culture time intervals was significantly influenced by the plasma-treated surface of nanofibers as well. This approach to modifying and controlling the surface properties of nanofibers could be promising in the design and tailoring of novel synthetic extracellular matrices for tissue engineering applications.

Acknowledgements

This research was supported by National Nature Science Foundation of China (project No. 31070871, 31271035), National High Technology Research and Development Program (863) (project No. 2008AA03Z305), Science and Technology Commission of Shanghai Municipality (project No. 11nm0506200), the National Plan for Science and Technology (Grant 10NAN1013-02).

References

- [1] Y. Yang, M. Porte, P. Marmey, A.J. El Haj, J. Amedee, C. Baquey Nuel, *Instr. Method Phys. Res. B* 207 (2003) 165.
- [2] L. Jeong, I. Yeo, H.K. Kim, Y. Yoon, D.H. Jang, S.Y. Jung, B. Min, W.H. Park, *Int. J. Biol. Macromol.* 44 (2009) 222.
- [3] H.U. Lee, Y.S. Jeong, S.Y. Jeong, S.Y. Park, J.S. Bae, H.G. Kim, C.R. Cho, *Appl. Surf. Sci.* 254 (2008) 5700.
- [4] F. Rombaldoni, K. Mahmood, A. Varesano, M.B. Songia, A. Aluigi, C. Vineis, G. Mazzuchetti, *Surf. Coat. Technol.* 216 (2013) 178.
- [5] M.D. Schofer, U. Boudriot, S. Bockelmann, A. Walz, J.H. Wendorff, A. Greiner, J.R.J. Paletta, S. Fuchs-Winkelmann, *J. Mater. Sci. Mater. Med.* 20 (2009) 1537.
- [6] Y. Wan, J. Yang, J. Yang, J. Bei, S. Wang, *Biomaterials* 24 (2003) 3757.
- [7] T. Jacobs, R. Morent, N.D. Geyter, P. Dubruel, C. Leys, *Plasma Chem. Plasma Process.* 32 (2012) 1039.
- [8] H. Xu, R. Deshmukh, R. Timmons, K.T. Nguyen, *Tissue Eng. A* 17 (2011) 865.
- [9] M. Nakagawa, F. Teraoka, S.F. Jimoto, Y. Hamada, H. Kibayashi, J. Takahashi, *J. Biomed. Mater. Res. A* 77 (2006) 112.
- [10] M.T. Khorasani, H. Mirzadeh, S. Irani, *Radiat. Phys. Chem.* 77 (2008) 280.
- [11] F. Teraoka, M. Nakagawa, M. Hara, *Dent. Mater. J.* 25 (2006) 560.
- [12] X.M. Mo, C.Y. Xu, M. Kotaki, S. Ramakrishna, *Biomaterials* 25 (2004) 1883.
- [13] Z. Gugala, S. Gogolewski, *J. Biomed. Mater. Res. A* 76A (2008) 288.
- [14] B.S. Jang, Y. Jung, I.K. Kwon, C.H. Mun, S.H. Kim, *Macromol. Res.* 20 (2012) 1234.
- [15] W. He, Z.W. Ma, T. Yong, W.E. Teo, S. Ramakrishna, *Biomaterials* 26 (2005) 7606.
- [16] P. Verdonck, P.B. Caliope, E.D.M. Hernandez, A.N.R. Silva, *Thin Solid Films* 515 (2006) 831.
- [17] J.P. Chen, C.H. Su, *Acta Biomater.* 7 (2011) 234.
- [18] K. Ma, C.K. Chan, S. Liao, W.Y.K. Hwang, Q. Feng, S. Ramakrishna, *Biomaterials* 29 (2008) 2096.
- [19] B. Maurina, P. Canadasa, H. Baudrillera, P. Montcourrier, N. Bettache, *Thin Solid Films* 41 (2008) 2036.
- [20] P. Roach, D. Eglin, K. Rohde, C.C. Perry, *J. Mater. Sci. Mater. Med.* 18 (2007) 1263.
- [21] B.M. Gumbiner, *Cell* 84 (1996) 345.
- [22] E.A. Voger, R.W. Bussian, *J. Biomed. Mater. Res.* 21 (1987) 1197.
- [23] F. Rosso, A. Giordano, M. Barbarisi, A. Barbarisi, *J. Cell. Physiol.* 199 (2004) 174.
- [24] D.E. Ingber, *J. Folkman, Cell* 58 (1989) 803.